ISSN 1330-3651 (Print), ISSN 1848-6339 (Online) https://doi.org/10.17559/TV-20230205000322
Preliminary communication

Application of High Density Resistivity Method in Karst Exploration: A Case Study

Xiandong WEI, Yang LIU*, Xinxin LI, Yulong LU

Abstract: During engineering and construction activities, water and mud burst, house and ground collapse, as well as other hazards often occur in places where karst develops, which can seriously threaten the safety of people's life and property and limit the development of local society and economy. Therefore, it is a meaningful work to figure out the locations of karst development so that corresponding prevention measures could be taken in advance. In this study, a case was introduced by using high density resistivity method to study the karst ground collapse. The geological characteristics, distribution law and control factors of karst ground collapse were clarified through high density resistivity method. Based on the results, the development trend was predicted, and the corresponding treatment measures and suggestions were proposed. The results show that 2 karst developing belts and 3 karst seriously-developed centers were delineated in the study region, which indicates that the high density resistivity method can effectively identify abnormal underground areas in the study region. The results shown in this research would provide the whole site for future drilling and the useful experience for underground karst exploration in similar areas.

Keywords: high density resistivity method; karst collapse; karst zone

1 INTRODUCTION

With the advancement of society and technology, the scope of human activities is expanding constantly. Even if the geological conditions of some construction sites are not good enough, such as some production venues and residential buildings are constructed in areas where geological disasters are developing, still we can make use of modern technologies to treat and control these unfavourable conditions.

The study region is at the Zhadu Town Resident Committee of Lengshuijiang City, Loudi City, Hunan Province, China, karst ground collapse occurs on an unstable slope. By consulting local residents, it is known that some brick houses built on the slope cracked a few years ago, and the widest crack reaches 7 cm. To analyze the karst ground collapse at the site, study the influence scope of the hazard, and provide evidence for drilling construction, before the drilling work, the high density resistivity method was used to explore the karst.

Geophysical research was conducted to figure out the development history, status, cause, type, formation condition, geological pattern, and spatial distribution law of karst ground collapse in the study region, then, the main factors that control the karst ground collapse could be determined, and the development trend of underground karst that causes the ground collapse and its threats to surrounding areas could be predicted, further, relevant measures and suggestions could be proposed to control un-happened karst ground collapse, eliminate and treat the happened karst ground collapse, and protect the collapsed ground.

The high density resistivity method is a geophysical exploration technique proposed in the late 1970s. At that time, the conventional electrical methods were time-consuming and their performance was unsatisfactory in real applications [1-4]. In the mean time, because manual operations are prone to generating interference and errors, scholars came to the idea of designing a large-array electrical exploration system, and the electrical sounding bias system designed by British geophysicists is actually the original mode of the high density resistivity method in electrical exploration [5-8]. In the mid 1980s, the electrode conversion board was used to realize the collection of field data for the first time. However, due to the limitations of the required technologies and the system design at that time, the advantages of this equipment in other aspects have not been shown yet [9, 10].

In China, the high density resistivity method was developed gradually since the late 1980s [11]. Since then, the Chinese government has begun to pay attention to geological survey, and field scholars have increased understandings of the geophysical exploration methods. Per the requirements of various engineering and construction works in the country, the Ministry of Geology and Mineral Resources took the lead in carrying out research on high density resistivity method and its applications [12-15]. In both theory and practice, field scholars have discussed this method and solved a few difficulties related to it, also, some devices that fit the requirements at that time have been developed according to these research achievements [16-18].

Now the high density resistivity method is a mature geophysical exploration method that has been widely used in geological survey and many engineering exploration fields including the detection of goaf areas, ground cracks, and underground karst areas [19, 20]; the application effect in these projects is satisfactory, as a result, the economic benefits of local society have been improved. The high density resistivity method provides important theoretical evidences and technical support, and it makes the arrangement of related works more reasonable and smooth.

2 METHOD

2.1 Traffic and Geological Location

Zhadu Town is located in the northeast suburb of Loudi City, 35 km away from the downtown. Zhadu Town covers an area of about 43 km^2 and has a population of more than 25000, 13 village committees and Limin Coal Mine Area next to Zhadu. The study region is located at 111°57' east longitude and 27°72' north latitude; within the study region, there is a 10000 volt substation that can supply sufficient power. The postal service and telecommunications in the study region are good, the infrastructure facilities are complete, and the transportation

is convenient, as shown in Fig. 1.

2.2 Geophysical Features

According to the geological data collected before and the information attained during site survey, it is known that the strata in the study region are mainly the Quaternary Holocene miscellaneous layer (Q_4^{ml}), the Quaternary eluvial and diluvial layer (Q^{el+dl}), and the lower Carboniferous Datangian stage Shidengzi limestone (C_1d^l).

The Quaternary soil mass in the study region mainly has two types: the Quaternary planting deposits (QPD) and silty clay (QAL), although the resistivity of the two is low, still the water content of local soil mass may be lower than that of surrounding soil, and this non-uniformity might lead to high resistance in local observation data. According to previous experience, the range of resistivity is shown in Tab. 1; there are certain differences in the resistivity, and the geophysical conditions for carrying out geophysical exploration works are met.

The resistivity of a complete limestone is about 1000 Ω·m ~ 2000 Ω·m. In case that there are karst developing belts in the limestone stratum, physical spaces such as fractures are inevitable; once they are filled by mud, sand, or water, the resistivity will be lower than surrounding rocks, in geophysical exploration, it exhibits as low resistivity abnormality.

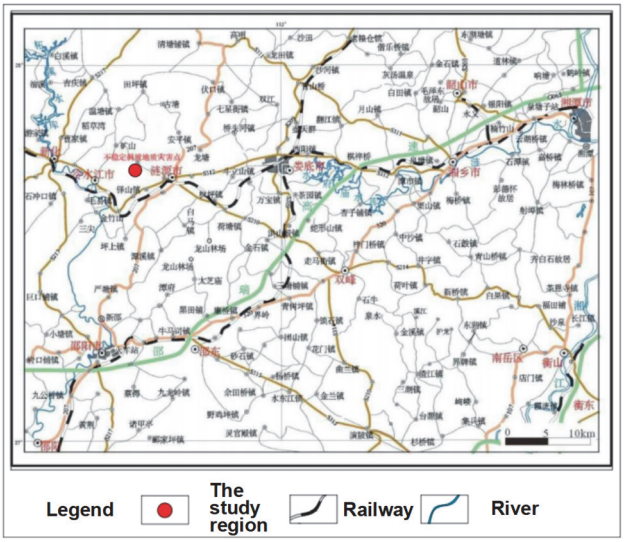

Figure 1 Traffic and location of Zhadu Town

Table 1 Electrical parameters of lithology

Lithology	Measurement method	Range of resistivity / Ω·m	Common resistivity/ Ω·m
Clay		$1 \sim 10^2$	30
Siltstone	Mini four electrode array on outcrops	5×10^2	200
Limestone	Mini four electrode array on outcrops	1×10^3	2000
Karst collapse	Data collection	$1 \sim 10^2$	50

2.3 Method Selection for Karst Detection

The detection of hidden karst collapse mainly relies on the geophysical exploration. The technical principle of seismic exploration is based on the differences of kinematic and dynamic characteristics of seismic wave propagation in stratum interface structure and media with different physical characteristics [21-23]. However, seismic exploration is easily affected by strong human interference, and obtaining high-quality data requires explosive sources, which may cause damage to the surrounding environment [24, 25]. Geological radar method is a shallow geological advance prediction method, which uses the difference between the length of electromagnetic wave propagation time in the transport medium to determine the properties and occurrence of the geological body. However, the detection depth of high-frequency electromagnetic wave is only a few meters, which cannot meet the exploration requirements of karst collapse [26, 27]. Electrical exploration is a geophysical exploration method that uses manually input direct or alternating current (magnetic) fields to study geological structures and find minerals based on the different electrical or electromagnetic properties of underground rocks or ores. The resistivity method is a direct current (DC) exploration method developed based on the different conductivity of various rocks or ores in the crust. When DC is manually applied to the ground, the distribution of ground electric field can be observed by instruments on ground surface. Then by studying the distribution law of such artificial electric field, the spatial positions with non-uniform resistivity underground can be found, the positions and approximate depths of the geologic bodies can be determined, ultimately, the underground minerals can be found and the geological problems can be solved [28-30]. According to the karst exploration requirements and the geophysical features of the study region, the high density resistivity method has been adopted in this research.

Principle of this high density resistivity method is not a brand-new theory, actually it is the same as that of the conventional resistivity method, but there are some differences between the two [31, 32]. The conventional resistivity method uses a total of four electrodes: two input current electrodes and two receiving current electrodes. During actual use, once the measurement of a group of profiles has been completed, the electrodes need to be moved manually, so it is prone to errors or deviations caused by manual operations. The number of electrodes required by the highdensity resistivity method is uncertain, dozens or hundreds of electrodes may be required according to actual conditions. During actual use, the electrodes need to be manually arranged at pre-set positions at one time, then the instruments required by the high density resistivity method were connected for direct observation, during which there is no need to move the electrodes manually. The observation instruments can control the electrodes automatically, in this way, automation or semi-automation could be realized, and such difference in actual application gives the high density resistivity method a series of advantages compared with the conventional resistivity method, including low cost, high efficiency, rich data information, and easier abnormality interpretation.

2.4 Selection of Instruments for the High Density Resistivity Method

According to the karst geological characteristics and the surface features of the study area, 5 northeast-oriented survey lines and 3southwest-oriented survey lines were set across the whole area. The layout of the survey lines is shown in Fig. 2.

In this study, the high density resistivity method selected α arrangement, namely the Wenner4 probe tester. When conducting field observation in the study region, the spacing between AM, MN and NB was equal, and this distance was taken the spacing between electrodes (electrode spacing). Starting from one end of a survey line, the four points A, M, N and B moved in one direction one by one; when they reached the other end of the survey line, the first profile could be attained. Then, the spacing between AM, MN and NB was increased by one electrode spacing, and the four points A, M, N and B again started from one end of another survey line and moved in one direction one by one until reaching the other end of this survey line, then another profile could be attained. In this way, the scanning and measurement continued to get an inverted trapezoidal profile. In this study, 5 m was selected as the spacing between electrodes, 60 electrodes were arranged on each survey line, when the same survey line had rolled for 58 times, a profile was attained. The profiles had a total of 10 layers. 8 survey lines were set, for each survey line, the east, north and northeast directions were numbered with Roman numerals.

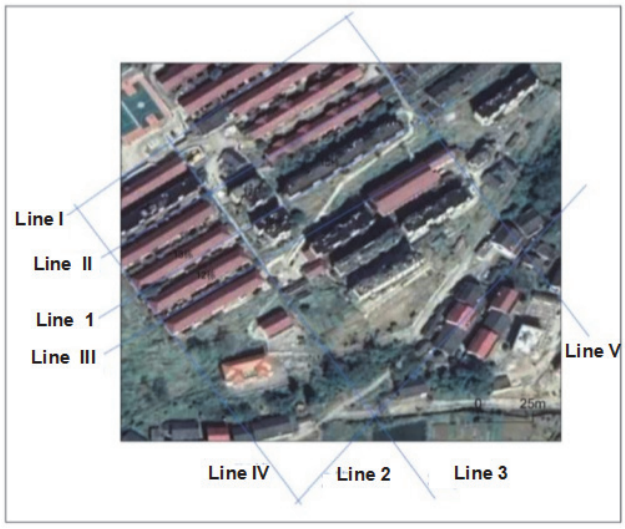

Figure 2 Layout of survey lines in the study region

2.5 Field Observation

During the karst exploration, when the high density resistivity method was adopted for site observation, attentions should be paid to whether the data collected by the instruments on site have negative numbers or distortion points. If the data displayed on the instruments show negative numbers or distortion points, in most cases, they are caused by the poor grounding conditions of some electrodes. If this situation occurs during site observation, then it is necessary to immediately stop the observation and check the grounding conditions of electrodes; once the data return to normal, the observation could be continued. During site observation, if a data collector finds that the current data or voltage data displayed by the data collection instrument are too small that they can affect the observation results, then at this time, the power supply voltage of the instrument needs to be increased, and the measurement should be taken again after the increased voltage is stabilized, and the observation could be continued once all observation data are normal.

2.6 Instruments and Quality Review

The instruments used during karst exploration are a model WDJD-3 multifunctional digital DC excitation meter and a model WGMD-3 highdensity resistivity measurement system. The two instruments were both developed by the Chongqing Benteng Digital Control Technical Institute.

To ensure the data quality of site observation in the study region, during the everyday works on the site, the operation manuals of instruments and the technical specifications of field observation were strictly followed. Moreover, repeated observations had been taken as self-checking method in the karst exploration, and the same profile was observed by different operators for repeated observations and cross-checking; these two methods were adopted at the same time to ensure the reliability of the karst exploration works.

Since only one set of instruments had been used during the hydrological exploration, the work quality check selected to use the same instrument at the same site during different time periods and operated by different operators, and the quality check of hydrological exploration in the study region followed the principle of "two same and two different". In the mean time, in view of the difficulty of setting electrodes in the study region and the consistency required by observation points, the hydrological data were collected under the conditions of different power supply times, different power supply voltages, and different observation parameters. By comparing, the forms and features of the two are almost the same, indicating the high similarity between the two, and the instruments used for hydrological exploration were in a normal working state.

3 RESULTS AND DISCUSSIONS

3.1 Profile Interpretation

A total of 8 survey lines were arranged in the study region, 5 of which in the east-west direction and named Line I, Line II, Line 1, Line III, and Line 2; lines in the west were numbered with Arabic numerals, and the lines in the east were number with Roman numerals; 3 survey lines were arranged in the south-north direction, from west to east, there were Line IV, Line 3 and Line V; lines in the south were numbered with Arabic numerals, and lines in the north were numbered with Roman numerals, as shown in Fig. 2.

Survey line I was located at the northernmost part of the study region, the profile inversion is shown in Fig. 3a. The low resistivity layer on top of the inversion diagram shows the Quaternary planting deposits (QPD) and silty clay (QAL), and the thickness of soil layer of the two varies from 1m to 3m. There is a strip-shaped low resistivity belt under survey points 115 - 215 on the survey line, which has

the features of karst valley, overall, the abnormality exhibits as the shape of a bottleneck, and it is inferred that at the position of this low resistivity belt the cracks develop well; there is a higher resistivity layer on top of the low resistivity belt at the bottom, which is an uneven stress layer that is presented as a formation model that is harder on top and softer at bottom.

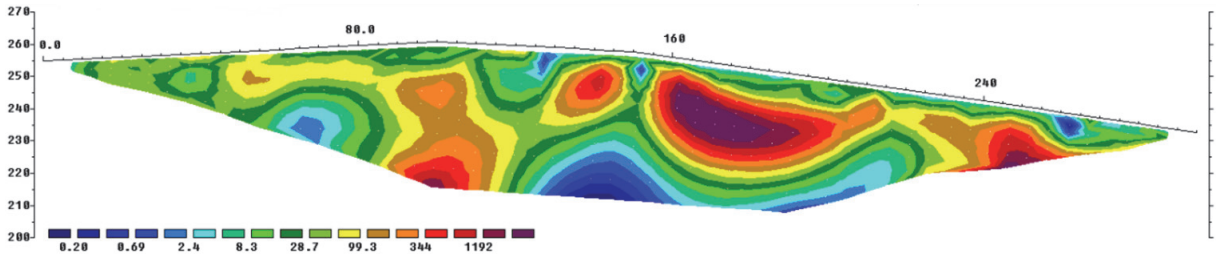

(a) Profile inversion

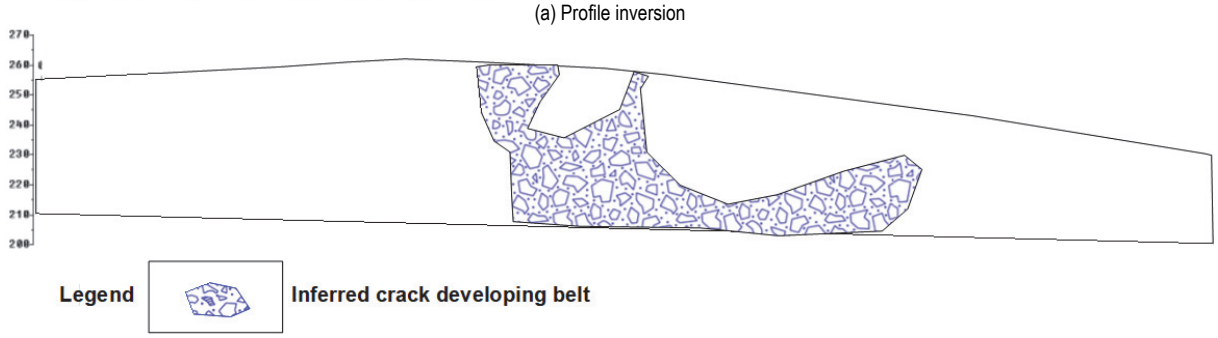

(b) Inferred results

Figure 3 Survey results of Line I in the study region

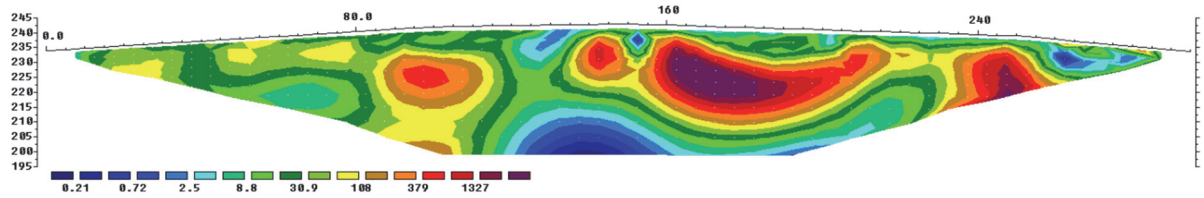

(a) Profile inversion

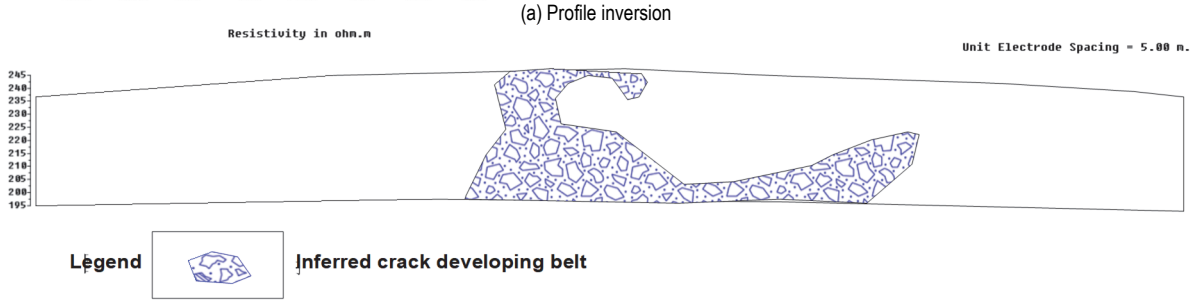

(b) Inferred results

Figure 4 Survey results of Line II in the study region

Survey line II was located near the school in the north-central part of the study region, its profile inversion is shown as Fig. 4a, which is similar to the observation result of the profile of survey line I, indicating that the two are highly similar and both are continuous. The low resistivity layer on top of the inversion diagram reflects the Quaternary planting deposits (QPD) and silty clay (QAL), and the thickness of soil layer of the two varies from 1m to 3m. Beneath survey points 115 - 215 on survey line II, there is a belt-shaped low resistivity layer that has the features of karst valley. On the whole, the abnormality shows as a bottleneck shape, and it is inferred that cracks are developing at the position of this low resistivity belt. There is a higher resistivity layer on top of the low resistivity belt at the bottom, which is an uneven stress layer that is presented as a formation model that is harder on top and softer at bottom. On top of the low resistivity layer at the bottom, there is an uneven-stress higher resistance layer which is presented as a formation model that is harder on top and softer at bottom.

Survey line 1 was located between the No.13 and No.16 buildings of the Limin community in the study region, its profile inversion is shown in Fig. 5a. The low resistivity layer on top of the inversion diagram reflects the Quaternary planting deposits (QPD) and silty clay (QAL), and the thickness of soil layer of the two varies from 1 m to 3 m. Under the survey points 145 - 155 on this survey line, there is a low resistivity belt with the features of karst valley. The abnormality is shown as a bottleneck shape, and it is inferred that cracks are developing at the position of this low resistivity belt, which is prone to stress imbalance that causes shear damage to ground buildings above this position. At the same time, there is also a low resistivity abnormality in the shallow part between survey points 175 - 195 on this survey line, and it is inferred that small cracks are developing under this abnormality area.

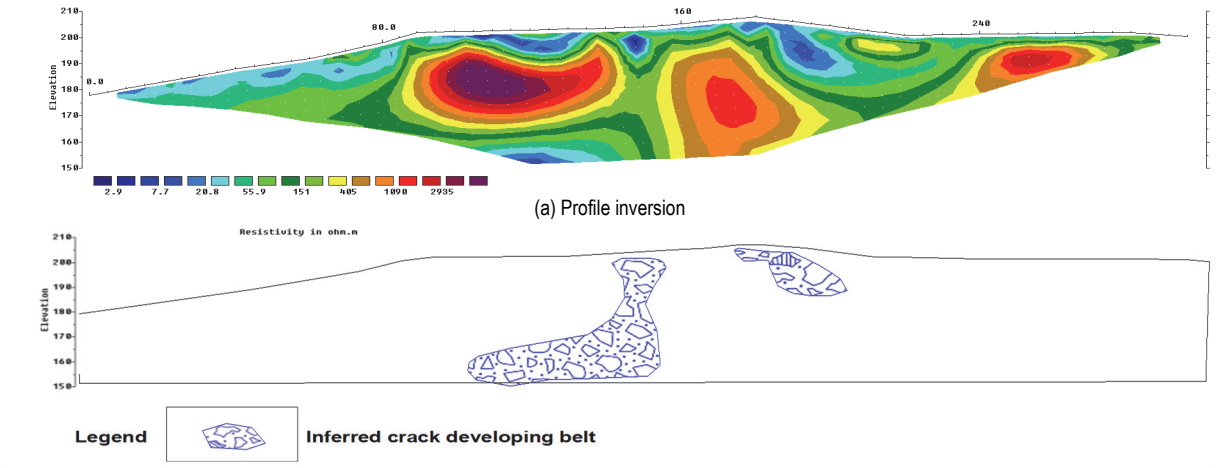

(a) Profile inversion

(b) Inferred results

Figure 5 Survey results of Line 1 in the study region

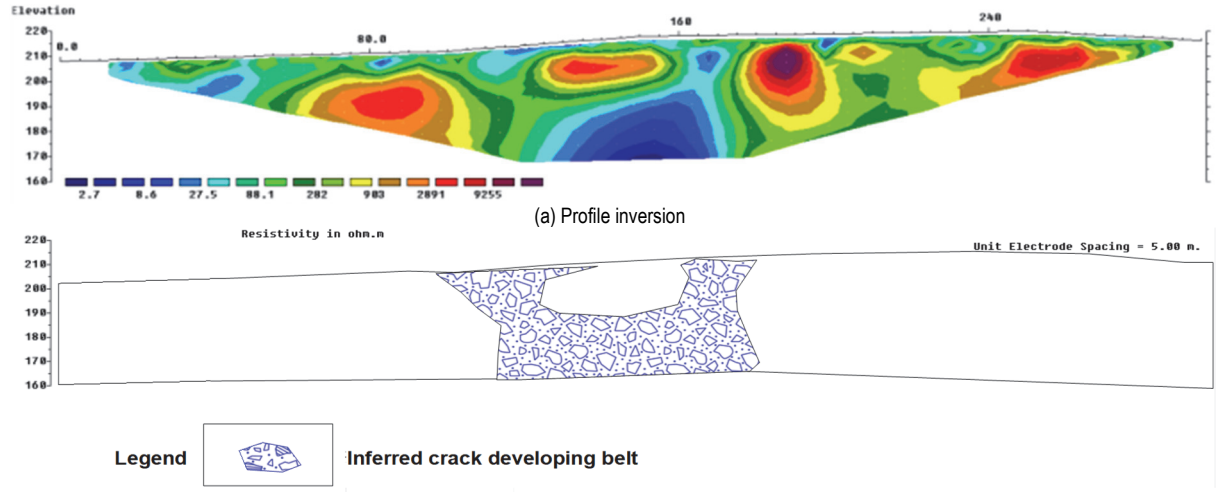

(a) Profile inversion

(b) Inferred results

Figure 6 Survey results of Line III in the study region

Survey line III was located in the south of No.12 building of Limin community in the study region, and its profile inversion is shown in Fig. 6a. The low resistivity layer on top of the inversion diagram reflects the Quaternary planting deposits (QPD) and silty clay (QAL), and the thickness of soil layer of the two varies from 1 m to 3 m. In the deeper part between survey points 120 - 185 on this survey line, there is an extremely low resistivity abnormality area, and the east-west direction profile is the largest in terms of both depth and width, and it is inferred that this is the biggest abnormality area in the study region.

Survey line 2 was located in the south of the residential area of Limin Coal Mine in the study region, the nearby walls show obvious deformations, and the profile inversion in shown in Fig. 7a. The low resistivity layer on top of the inversion diagram reflects the Quaternary planting deposits (QPD) and silty clay (QAL), and the thickness of soil layer of the two varies from 1m to 5m. Beneath the survey points 150 - 175 on this survey line, there is a valley-shaped low resistivity abnormality area. This abnormality has a large scale, and its overall shape is conical. It is inferred that the low resistivity abnormality belt between survey points 145 - 155 on this survey line is consecutive. In the mean time, there is also a low resistivity abnormality area beneath survey points 190 - 220, the overall shape of this abnormality area is a belt, and it is connected with the shallow area under survey points 175 - 195 on this survey line. It is inferred that there are karst and cracks developing in the underlying bedrock.

There were three survey lines in the east-west direction, which were Line IV, Line 3, and Line V from west to east, the line in the south was numbered with Arabic numerals, and the lines in the north were numbered with Roman numerals.

The profile inversion of survey line IV is shown in Fig. 8a. According to the inversion diagram, overall speaking, the survey line is the area with the smallest abnormality range within the study region, there is a low resistivity belt with a deeper going tendency and a narrow range.

The survey line 3 was arranged basically orthogonal to survey line 1 and survey line 2 to measure the distribution of the conical abnormality valley of two profiles along the landslide direction, and the profile inversion is shown in Fig. 9a. The low resistivity layer on top of the inversion diagram reflects the Quaternary planting deposits (Q_{pd}) and silty clay (Q_{al}), and the thickness of soil layer of the two varies from 2 m to 6 m. This profile shows that the area between survey points 85 - 185 is the position with the greatest abnormality in the residential area. The crack abnormality is distributed between survey points 140 - 190 on this survey line, it extends deeper than the exploration

depth. The other abnormality is distributed between survey points 195 - 215 on this survey line, exhibiting as a conical valley.

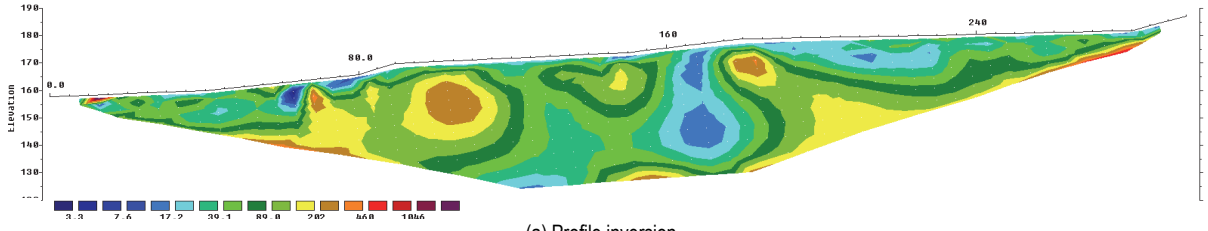

(a) Profile inversion

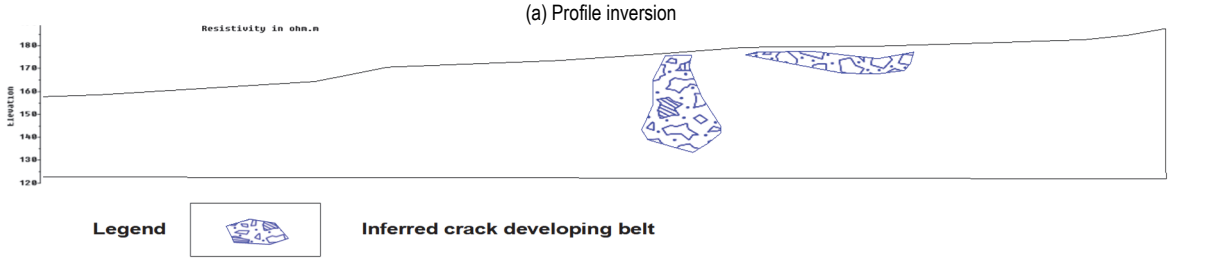

Legend Inferred crack developing belt

(b) Inferred results

Figure 7 Survey results of Line 2 in the study region

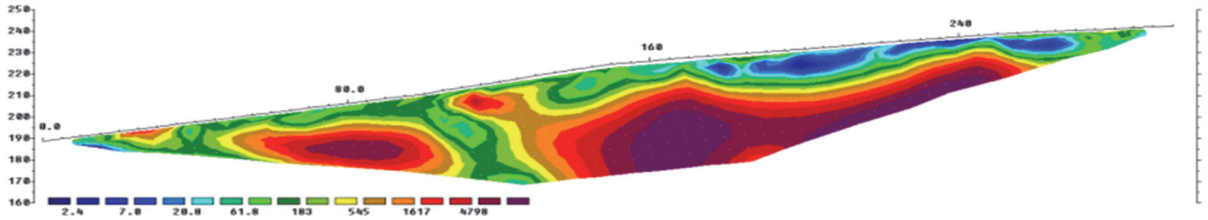

a) Profile inversion

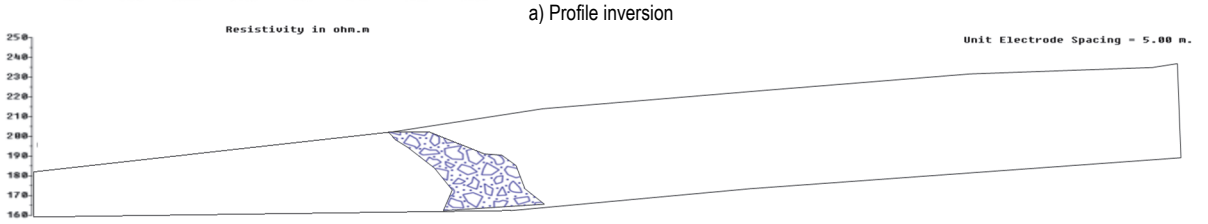

Legend Inferred crack developing belt

b) Inferred results

Figure 8 Survey results of Line Ⅳ in the study region

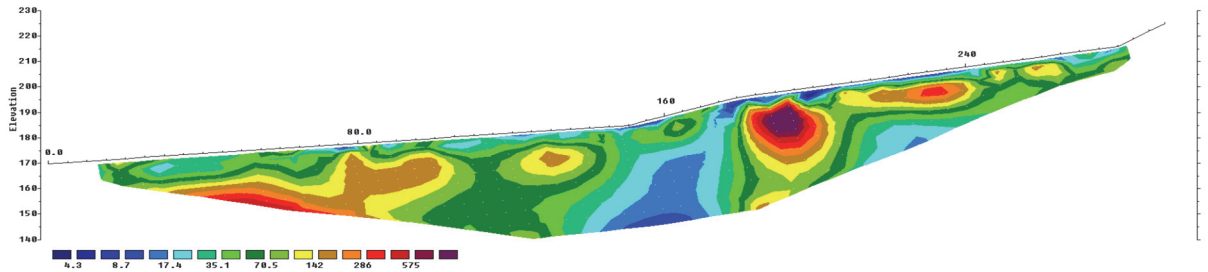

(a) Profile inversion

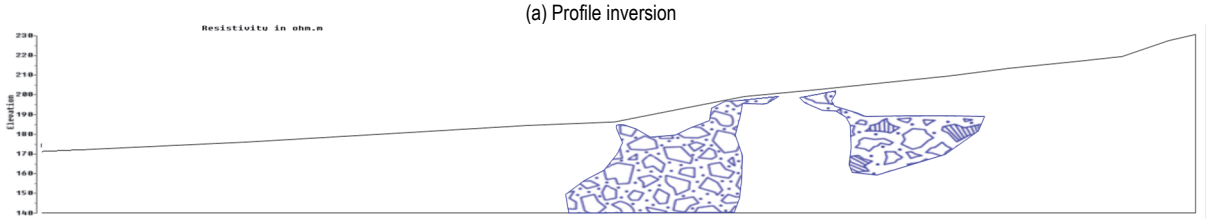

Legend Inferred crack developing belt

(b) Inferred results

Figure 9 Survey results of Line 3 in the study region

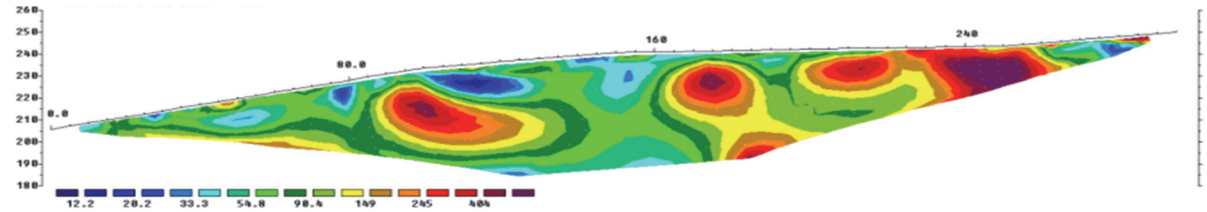

(a) Profile inversion

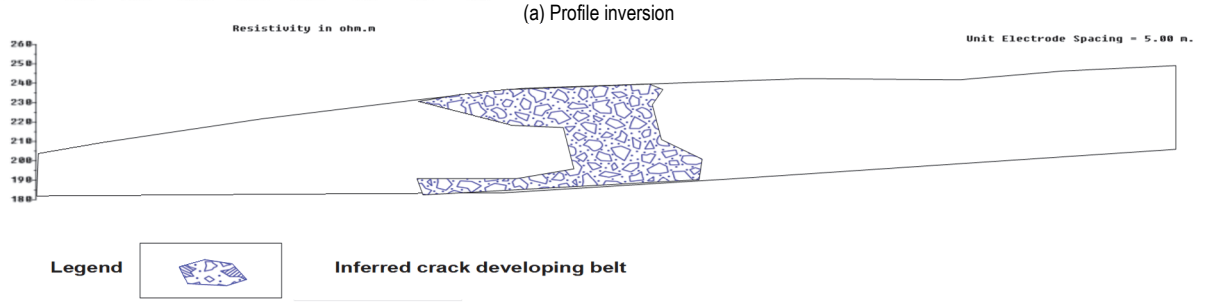

(b) Inferred results

Figure 10 Survey results of Line Ⅴ in the study region

Survey line V and survey line 3 were consecutive, and the profile inversion is shown in Fig. 10a. Between survey points 140 - 170 on this survey line, there is an abnormality with similar tendency and attitude.

3.2 Plane Interpretation

Combining with the inversion diagram of each survey line, on the whole, the survey lines in the east-west direction are consecutive. In the middle part of the 5 survey lines, there are hidden low resistivity belts of varying sizes, and there is also a suspected fault subsidence with a width ranging from 40 m to 70 m. The low resistivity belt starts from the position of the school in the north showing as a karst developing belt, and it grows the strongest near the No. 12 building, the other parts are mild karst developing areas, but on the whole, it shows a belt-shaped distribution in the south-north direction.

Figure 11 Plane interpretation of abnormalities in the study region

For survey lines running in the south-north direction, there is a very narrow abnormality belt on Line IV, the two survey lines in the east are consecutive, and there is an abnormality belt in the east-west direction, as shown in Fig. 11, the abnormality range is marked with red lines, and the abnormality concentration centers are circled by red ellipses as centers 1, 2, and 3.

3.3 Subsequent Works

(1) In the study region, the karst mainly develops in the lower Carboniferous Datangian stage Shidengzi limestone, and the reason is that the study region is a slope, the karst shows belt-shaped distribution, and the largest width of the abnormality area reaches about 60 m. Main cause of ground cracks is that the underground karst and water force have destroyed the original stratigraphic texture units, leading to unbalanced stress of the stratum. Moreover, the heavy and continuous rainfall and abundant groundwater in the study region have made the upper rock and soil layers saturated with water, which ultimately causes the deformation of the ground. If it is not treated for a long time, with the accumulation of days, the abnormality rang in the study region will grow, which can affect the daily life of residents. It is suggested to take maintenance measures such as setting up a fence at the lower part of the slope of the abnormality center 2.

(2) Combining with geological data and topographic conditions, it is suggested to determine the drill hole positions of the No. 150 survey point on survey line I, the No. 125 survey point on survey line II, the No. 160 survey point on survey line III, the No. 175 survey point on survey line 3, the No. 170 survey point on survey line 2, and the No. 15 survey point on survey line 1 for verification, so as to figure out the properties of abnormalities and accurately measure the karst abnormality and its affected range.

4 CONCLUSIONS

According to the survey results of the high density resistivity method, the geological data of the study region, and the on-site conditions, it can be inferred that:

(1) There are two abnormality belts within the study region, one belt runs from southeast to northwest, the other runs from east to west, and there are three abnormality centers in the study region. The first abnormality belt has the features that the geological hazard goes "weaker-stronger-weaker-stronger" from the south to the

north along the belt, and the abnormality range near the No.12 building in the Liming community and the school is larger than others in the belt; as for the second abnormality belt, it grows larger from the west to the east, so there is a possible tendency that the fault in the north would run through the abnormality center

(2) The abnormality belt running from southeast to northwest in the study region is the main abnormality area in this karst exploration. This abnormality belt shows an obvious concave state, and it is inferred that there is a local fault in the abnormality belt. The drilling verification based on the research results of this study would be conducted.

Acknowledgement

This work was supported by the Natural Science Foundation of Hunan Province (Grant No.: 2022JJ30244), the Research Project of Teaching Reform of Hunan Province (Grant No.: HNJG-2022-0790) and Xiangtan Key team project of science and Technology Innovation (Grant No.: ZY-CXTD20221003).

5 REFERENCES

[1] Komatina, S. M. (1994). Geophysical methods application in groundwater natural protection against pollution. *Environmental Geology*, *23*, 53-59. https://doi.org/10.1007/BF00773139

[2] Liu, Y., Bouazza, A., Gates W. P., & Rowe, R. K. (2015). Hydraulic performance of geosynthetic clay liners to sulfuric acid solutions. *Geotextiles and Geomembranes*, *43*(2), 14-23. https://doi.org/10.1016/j.geotexmem.2014.11.004

[3] Aleshin, I. M., Koryagin, V. N., Sukhoroslov, O. V., Kholodkov, K. I, & Shogin, A. N. (2011). Method of some inverse geophysical problem solution by using weakly coupled connected distributed computing systems. Automatic *Documentation and Mathematical Linguistics*, *44*(2), 302-304. https://doi.org/10.3103/S0005105510060051

[4] Liao, J., Guo, Z., Liu, H., Dai, S., Zhao, Y., Wang, L., Wang, H., & Andrew, H. (2017). Application of Frequency-Dependent Traveltime Tomography to 2D Crosswell Seismic Field Data. *Journal of Environmental and Engineering Geophysics*, *22*(4), 421-426. https://doi.org/10.2113/JEEG22.4.421

[5] Prates, J. H. S. & Moreira, D. M. (2020). Fractional derivatives in geophysical modelling: Approaches using the modified adomian decomposition method. *Pure and Applied Geophysics*, *177*(9), 430-4323. https://doi.org/10.1007/s00024-020-02480-6

[6] Amar, M., Maouedj, R., Atillah, A. B., Lorenzini, G., Ahmad, H., & Menni, Y. (2021). Design, construction and experimental testing of solar water heaters under Saharan weather conditions. *International Journal of Sustainable Development and Planning*, *16*(6), 997-1003. https://doi.org/10.18280/ijsdp.160601

[7] Fazlollahtabar, H. (2022). Mathematical Modeling for Sustainability Evaluation in a Multi-Layer Supply Chain. *Journal of Engineering Management and Systems Engineering*, *1*(1), 2-14. https://doi.org/10.56578/jemse010102.

[8] Liu, Y., Gates W. P., & Bouazza, A. (2019). Impact of acid leachates on microtexture of bentonites used in geosynthetic clay liners. *Geosynthetics International*, *26*(2), 136-145. https://doi.org/10.1680/jgein.18.00043

[9] Suharini, E., Kurniawan, E., & Syifauddin, M. (2022). Evaluating the implementation of BNPB's Srikandi Bencana program in Dharma Wanita PersatuanUNNES. *International Journal of Safety and Security Engineering*, *12*(3), 329-337. https://doi.org/10.18280/ijsse.120307

[10] Liu, Y., He, B., Xie, J., Lu, Y., & Zhang, L. (2021). Compatibility of geosynthetic clay liners at different temperatures. *Journal of Environmental Protection and Ecology*, *22*(6), 2295-2306.

[11] Ling, J., Dai, S., Zhou, Y., Chen, Q., Zhang, Y., & Li, K. (2022). Three-Dimensional DC Anisotropic Resistivity Modeling Using a Method in the Mixed Space-Wavenumber Domain. *Pure and Applied Geophysics*, *179*(6), 2183-2200. https://doi.org/10.1007/s00024-022-03043-7

[12] Ivorra, S., Bru, D., Galvañ, A., Silvestri, S., Apera, C., & Foti, D. (2017). Trm reinforcement of masonry specimens for seismic areas. *International Journal of Safety and Security Engineering*, *7*(4), 463-474. https://doi.org/10.2495/SAFE-V7-N4-463-474

[13] Tang, L., Tang, X., Liu, Y., & Qu, S. (2020). Prediction of pore size characteristics of woven slit-film geotextiles subjected to unequal biaxial tensile strains. *Geotextiles and Geomembranes*, *48*(5), 724-734. https://doi.org/10.1016/j.geotexmem.2020.05.005

[14] Dutta, S., Bardhan, S., Bhaduri, S., & Koduru, S. (2020). Understanding the relationship between density and neighbourhood environmental quality-a framework for assessing Indian cities. *International Journal of Sustainable Development and Planning*, *15*(7), 1067-1079. https://doi.org/10.18280/ijsdp.150711

[15] Jalali, A., Roös, P. B., Herron, M., Sidiqui, P., Beza, B., & Duncan, E. (2022). Modelling coastal development and environmental impacts: A case study across two regional towns in Australia. *International Journal of Design & Nature and Ecodynamics*, *17*(4), 491-501. https://doi.org/10.18280/ijdne.170402

[16] Liu, Y., Hao, Y., & Lu, Y. (2018). Improved Design of Risk Assessment Model for PPP Project under the Development of Marine Architecture. *Journal of Coastal Research*, *83*(S1): 74-80. https://doi.org/10.2112/SI83-013.1

[17] Rosenhouse, G. (2019). From nature and basic scientific results to modern engineering applications. International *Journal of Design & Nature and Ecodynamics*, *14*(4), 249-263. https://doi.org/10.2495/DNE-V14-N4-249-263

[18] Vulevic, A., Castanho, R. A., Gómez, J. M. N., & Quinta-nova, L. (2022). Tendencies in Land Use and Land Cover in Serbia Towards Sustainable Development in 1990-2018. *Acadlore Transactions on Geosciences*, *1*(1), 43-52. https://doi.org/10.56578/atg010106

[19] Zhou, L., Liu, X., Li, J., & Liao, J. (2021). Robust AVO inversion for the fluid factor and shear modulus. *Geophysics*, *86*(4), 471-483. https://doi.org/10.1190/GEO2020-0234.1

[20] El Chaal, R. & Aboutafail, M. O. (2022). Comparing Artificial Neural Networks with Multiple Linear Regression for Forecasting Heavy Metal Content. *Acadlore Transactions on Geosciences*, *1*(1), 2-11. https://doi.org/10.56578/atg010102

[21] Zhao, Y. L., Zhang, C. S., Wang, Y. X., & Lin, H. (2021). Shear-related roughness classification and strength model of natural rock joint based on fuzzy comprehensive evaluation. International *Journal of Rock Mechanics and Mining Sciences*, *137*, 104550. https://doi.org/10.1016/j.ijrmms.2020.104550

[22] Liu, X., Zhou, L., Chen, X., & Li, J. (2020). Lithofacies identification using support vector machine based on local deep multi-kernel learning. *Petroleum Science*, *17*(4), 954-966. https://doi.org/10.1007/s12182-020-00474-6

[23] Huang, G., Xu, Y., & Yi, X. (2020). Highly efficient iterative methods for solving linear equations of three-dimensional sphere discontinuous deformation analysis. *International Journal for Numerical and Analytical Methods in Geomechanics*, *44*(9), 1301-1314.

https://doi.org/10.1002/nag.3062
[24] Liu, Y., Li, X., Tu, Y., & Lu, Y. (2023). Mining leachates effect on the hydraulic performance of geosynthetic clay liners under different temperatures. *Water*, *15*, 1132. https://doi.org/10.3390/w15061132
[25] Huang, W., Gao, F., Liao, J., & Chuai, X. (2021). A deep learning network for estimation of seismic local slopes. *Petroleum Science*, *18*(1), 92-105. https://doi.org/10.1007/s12182-020-00530-1
[26] Li, C., Liu, J., Liao, J., & Hursthouse, A. (2020). 2D High-resolution Crosswell Seismic Traveltime Tomography. *Journal of Environmental and Engineering Geophysics*, *25*(1), 47-53. https://doi.org/10.2113/JEEG19-003
[27] Yang, T., Gao, Q., Li, H., Fu, G., & Hussain, Y. (2023). New insights into the anomaly genesis of the frequency selection method: supported by numerical modeling and case studies. *Pure and Applied Geophysics*, *180*(3), 969-982. https://doi.org/10.1007/s00024-022-03220-8
[28] Zheng, D., Yao, Y., Nie, W., Chu, N., & Ao, M. (2021). A new three-dimensional computerized ionospheric tomography model based on a neural network. *GPS Solutions*, *25*, 1-17. https://doi.org/10.1007/s10291-020-01047-1
[29] Shang, M., Xiong, D., & Zhang, H. (2022). Landslide displacement prediction model based on time series and mixed kernel function SA-SVR. *Journal of Engineering Geology*, *30*(2), 575-588. https://doi.org/10.13544/j.cnki.jeg.2021-0584
[30] Wei, L., Li, J., Liu, L., Huang, L., Zheng, D., Tian, X., Huang, L., Zhou, L., Ren, C., & He, H. (2022). Lithosphere ionosphere coupling associated with seismic swarm in the Balkan Peninsula from ROB-TEC and GPS. *Remote Sensing*, *14*(19), 4759. https://doi.org/10.3390/rs14194759
[31] Shi, L., Wang, Y., Qiu, M., Gao, W., & Zhai, P. (2019). Application of three-dimensional high-density resistivity method in roof water advanced detection during working stope mining. *Arabian Journal of Geosciences*, *12*(464), 1-10. https://doi.org/10.1007/s12517-019-4586-7
[32] Xie, J., Liu, Y., Lu, Y., & Hang, L. (2022). Application of the high-density resistivity method in detecting a mined-out area of a quarry in Xiangtan City, Hunan Province. *Frontiers in Environmental Science*, *10*, 1068956. https://doi.org/10.3389/fenvs.2022.1068956

Contact information:

Xiandong WEI, Mr., Undergraduate student
School of Earth Sciences and Spatial Information,
Hunan University of Science and Technology,
Xiangtan 411201, China
Email: 1841211839@qq.com

Yang LIU, PhD, Associate Professor
(Corresponding author)
School of Earth Sciences and Spatial Information,
Hunan University of Science and Technology,
Xiangtan 411201, China
Email: 1020143@hnust.edu.cn

Xinxin LI, Mr., Postgraduate student
School of Earth Sciences and Spatial Information,
Hunan University of Science and Technology,
Xiangtan 411201, China
Email: 952036317@qq.com

Yulong LU, PhD, Senior Engineering
School of Earth Sciences and Spatial Information,
Hunan University of Science and Technology,
Xiangtan 411201, China
Email: 1010106@hnust.edu.cn